



CGSN Site Characterization: Southern Ocean

Control Number: 3201-00007

Version: 1-03

Date: February 28, 2011

Prepared by: S. White, M. Grosenbaugh, M. Lankhorst, H.-J. Kim, S.H. Nam, U. Send, D. Wickman, S. Morozova, R. Weller

Coastal and Global Scale Nodes
Ocean Observatories Initiative
Woods Hole Oceanographic Institution
Oregon State University
Scripps Institution of Oceanography



Revision History

Version	Description	Originator	ECR No.	Release Date
1-00	Initial Release	S. White	1303-00074	June 2, 2010
1-01	Add Current profile data (1.2.1), Lagrangian length scale data (1.2.5), Historical wind and wave data (1.3.1, 1.3.2), and Solar radiation data (1.3.4)	S. White	1303-00109	September 8, 2010
1-02	Added Argo float velocity data	M. Lankhorst		
1-03	Update current data, editorial updates	M. Lankhorst H.-J. Kim	1303-00224	February 28, 2011

Table of Contents

Scope	4
Overview	4
1. Site Survey.....	5
1.1. Bathymetry.....	5
1.1.1 Bathymetry Data.....	5
1.1.2 Bottom Type	6
1.2. Oceanographic Conditions	6
1.2.1 Currents.....	6
1.2.2 Mean Dynamic Ocean Surface Topography	12
1.2.3 Sea Surface Height Variability.....	14
1.2.4 Baroclinic Rossby Radius.....	14
1.2.5 Lagrangian Length Scale from Surface Drifters	15
1.3. Environmental Conditions.....	16
1.3.1 Historical Wind Data.....	16
1.3.2 Historical Wave Data.....	18
1.3.3 Weather Extremes.....	20
1.3.4 Solar Radiation.....	20
1.4. Commercial/Policy Factors	23
1.4.1 Shipping Lanes.....	23
1.4.2 Fishing Areas	24
1.4.3 Seafloor Cables.....	24
1.4.4 Other Moorings.....	24
1.4.5 Satellite altimetry tracks	25
2. Site Design.....	26
2.1. Site Components.....	26
2.2. Site Configuration	26
2.2.1 Moored Array.....	26
2.2.2 Glider Operations Area.....	29
3. References.....	30
Appendix A. Methodology for determining extreme events	31
Appendix B. Data sources	33

Southern Ocean Global Observatory Site Characterization

Scope

This report describes conditions in the atmosphere, in the ocean, and on the sea floor in the vicinity of the OOI Southern Ocean Array, and the infrastructure components and the proposed layout of the components at the site.

Overview

The selection of the sites for the global arrays was driven by the goal of establishing a few key stations in the data-sparse high latitudes that would provide sustained sampling at critical locations.

The Southern Ocean Global Observatory site is located at 55° S, 90° W southwest of Chile. The water depth is nominally 4800 meters. The mooring array will consist of one Global Surface Mooring with high-power and high-bandwidth data transmission, one Global Hybrid Profiler Mooring, and two sub-surface Global Flanking Moorings. The moored array will be complemented by 3 ocean gliders.

The four moorings and the gliders give the array the capability to address the role of the mesoscale flow field in ocean dynamics. Mesoscale features such as eddies not only have enhanced horizontal transports associated with their flow, but they also can modulate and increase mixing in the water column and vertical exchange with the atmosphere. Because of the importance of the mesoscale context, the spacing of the moorings reflects the scale of mesoscale variability at this latitude as quantified by the Rossby radius and the siting of the array takes into account overpasses of satellites with altimeters which will provide complimentary observations of the mesoscale and larger scale flows in the region.

The Southern Ocean site was chosen for its strong atmospheric forcing, strong winds and waves. A succession of strong storm systems typically move west to east through the region, and this site would be excellent for the study strong atmospheric forcing. One consequence of the winter-time forcing is the modification of surface water and convection. Antarctic Intermediate Water (AAIW) is formed there (England et al, 1993), and the formation mechanisms are the subject of a recent expedition to the area around the site (<http://www-pord.ucsd.edu/~ltalley/aaiw/> [1]). With the strong convection, atmospheric carbon dioxide in the surface layer enters the interior of the ocean in this region. Though Sabine et al.'s (2004) map of total air-sea carbon dioxide flux shows a modest sink at this site, the accompanying map of the inventory of anthropogenic carbon dioxide locates this site within a band of higher concentrations.

The site was also chosen to provide a contrasting biological regime. Compared to the Argentine Basin site there is little productivity as evidenced by ocean color. It is believed that low nutrient levels govern productivity at this site.

The site planning has taken into account developing oceanographic interests and the potential for collaboration in Chile. A Chilean plan for an Ocean South Pacific Array (OSEPA) (see http://ioc.unesco.org/goos/MS/rpts/Chil_R99.htm, [2]) would be complemented by the OOI Southern Ocean Site.

1. Site Survey

1.1. Bathymetry

1.1.1 Bathymetry Data

Bathymetry for the global sites was obtained from the Smith and Sandwell global database [3].

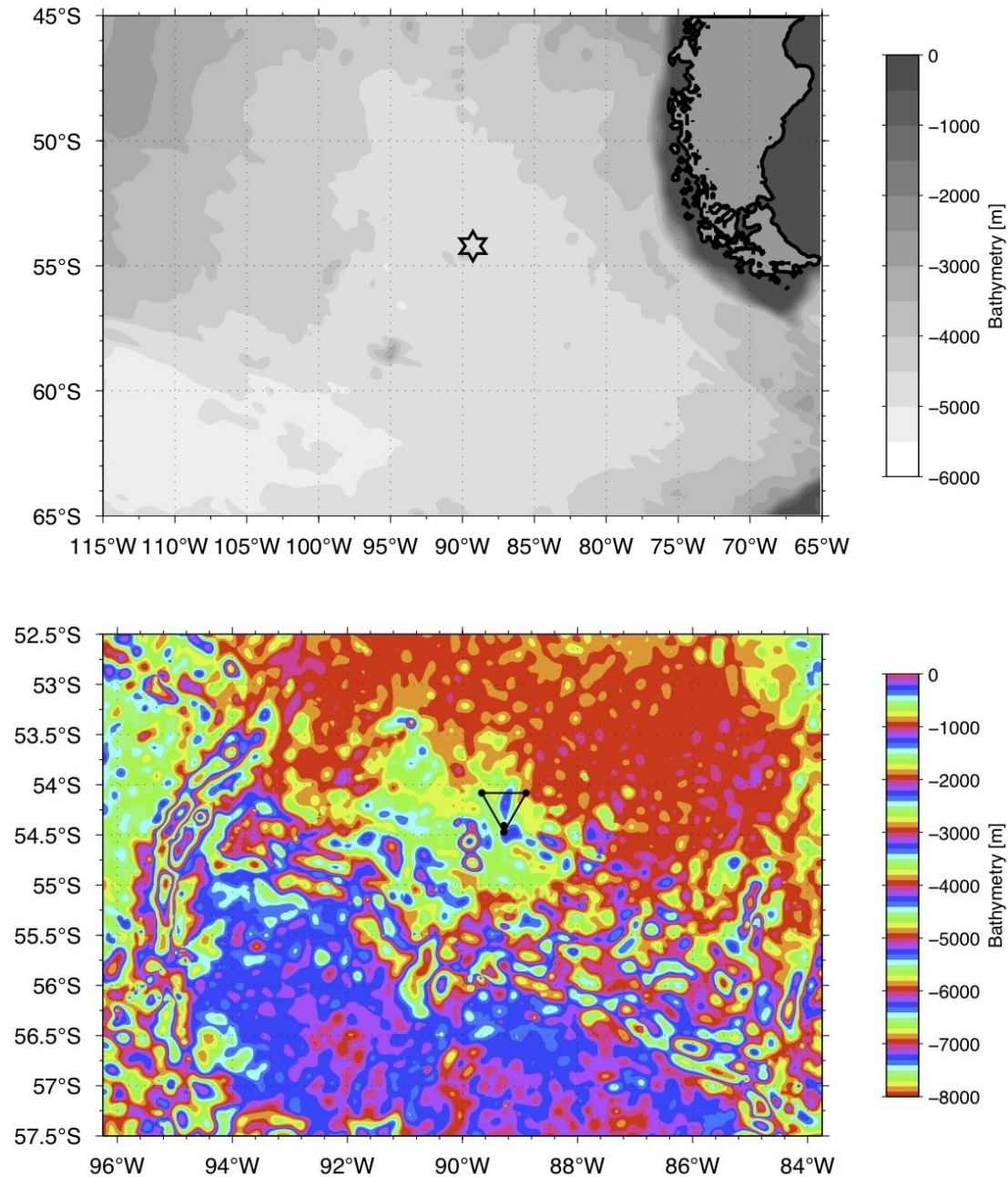


Figure 1. Smith & Sandwell Bathymetry [3] for the Southern Ocean Global Array site. Top: Contours every 500 m. Bottom: Close-up with contours every 100 m.

1.1.2 Bottom Type

We currently do not have any detailed data on bottom type in this region.

1.2. Oceanographic Conditions

1.2.1 Currents

1.2.1.1 In-Situ Data

Mooring Data:

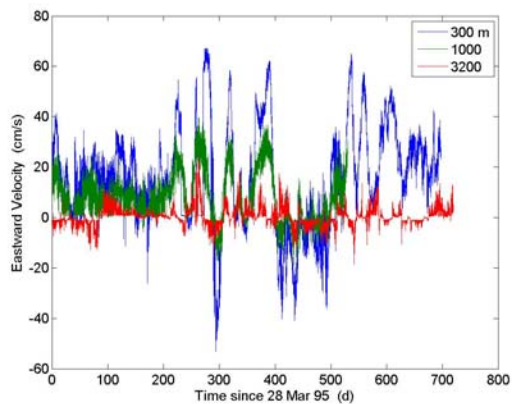


Figure 2a. E-W current velocity.

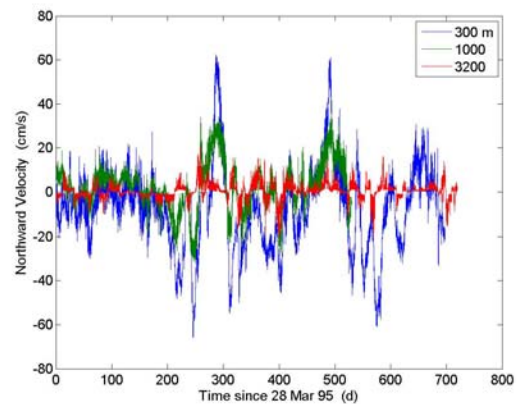


Figure 2b. N-S current velocity.

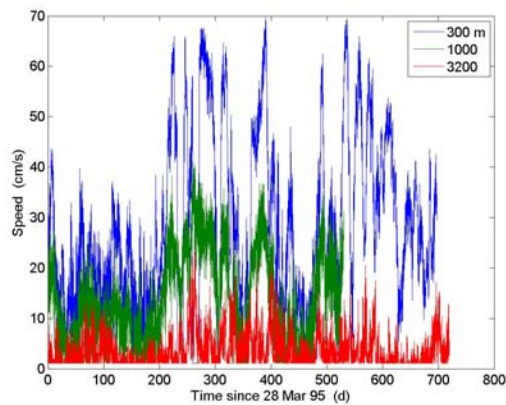


Figure 2. Current data from CSIRO mooring.

Figure 2c. Current speed.

Figure 2 gives current data from a mooring deployed by CSIRO in March 1995, at 50.7° S, 143.25 E south of Australia. This mooring was in the general path of the Antarctic Circumpolar Current (ACC). The shallowest current meter is at nominally 300 meters. The data are given

every 2 hours. It was not clear if this is instantaneous or average over 2 hours, but it should not make much difference (Jim Ledwell, personal communication). The maximum speed is 70 cm/s at 300 meters. Speeds at 1000 m are about half as great, and quite smaller at 3200 m. The actual OOI Southern Ocean site is located at 55° S, 90° W near the tip of South America, but is similarly affected by the ACC (Figure 3).

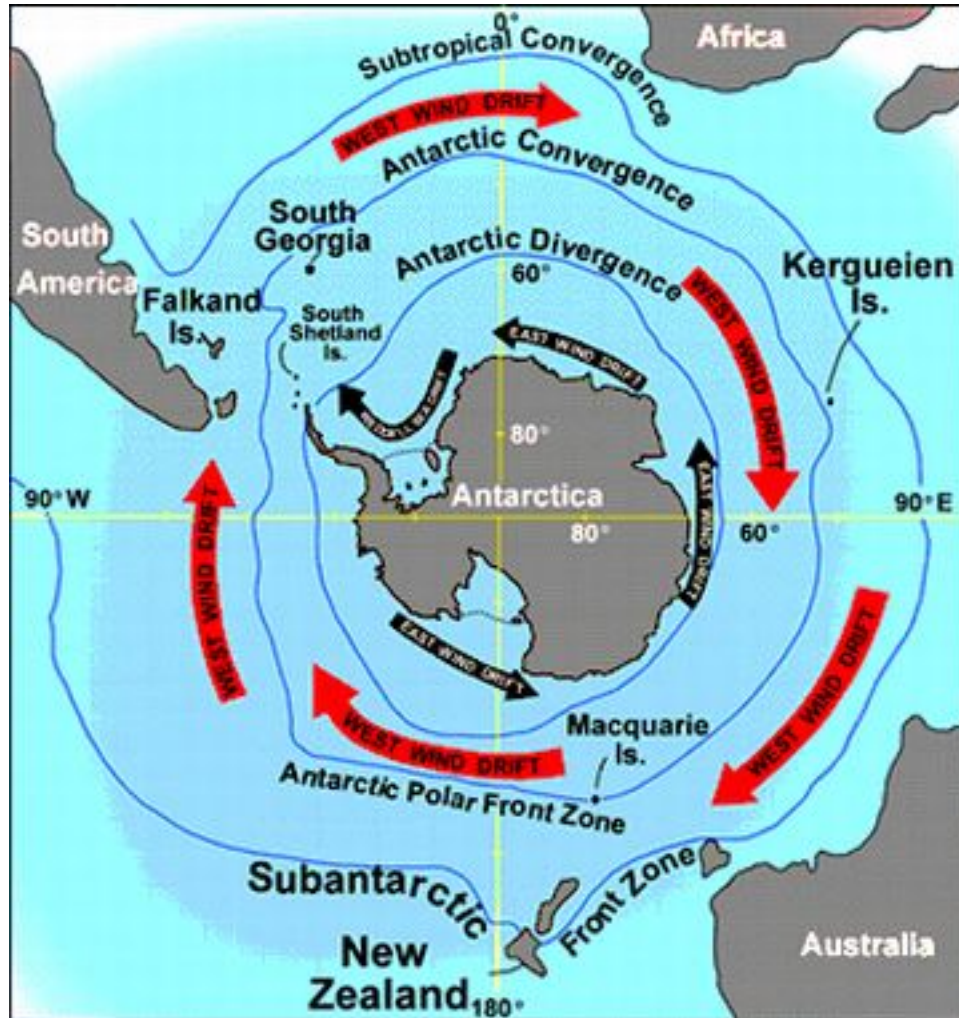


Figure 3. Red arrows show general circulation due to the Antarctic Circumpolar Current.

Surface Drifter Data:

The following are statistics derived from nearby surface drifter data. The data were obtained from <http://www.aoml.noaa.gov/envids/gld/> [4].

- Gaussian-weighted mean current vector : ... 13 cm/s (toward 91.3 deg.)
- Gaussian-weighted mean speed:..... 20 cm/s
- arithmetic mean current vector:..... 13 cm/s (toward 95.9 deg.)
- arithmetic mean speed:..... 20 cm/s

- std. dev. of east-west current: 14 cm/s
- std. dev. of north-south current: 14 cm/s
- std. dev. of current speed:..... 14 cm/s
- number of observations:..... 1275
- maximum current speed:..... 68 cm/s

Argo Float Data:

The subsurface current variability is characterized with Argo float data. Figure 4 shows statistics of temporal variability of subsurface currents. Each data point represents a ten-day average current derived from Argo float displacements over this time interval. Data are available at the Argo data centers (<http://www.argo.ucsd.edu> [5]).

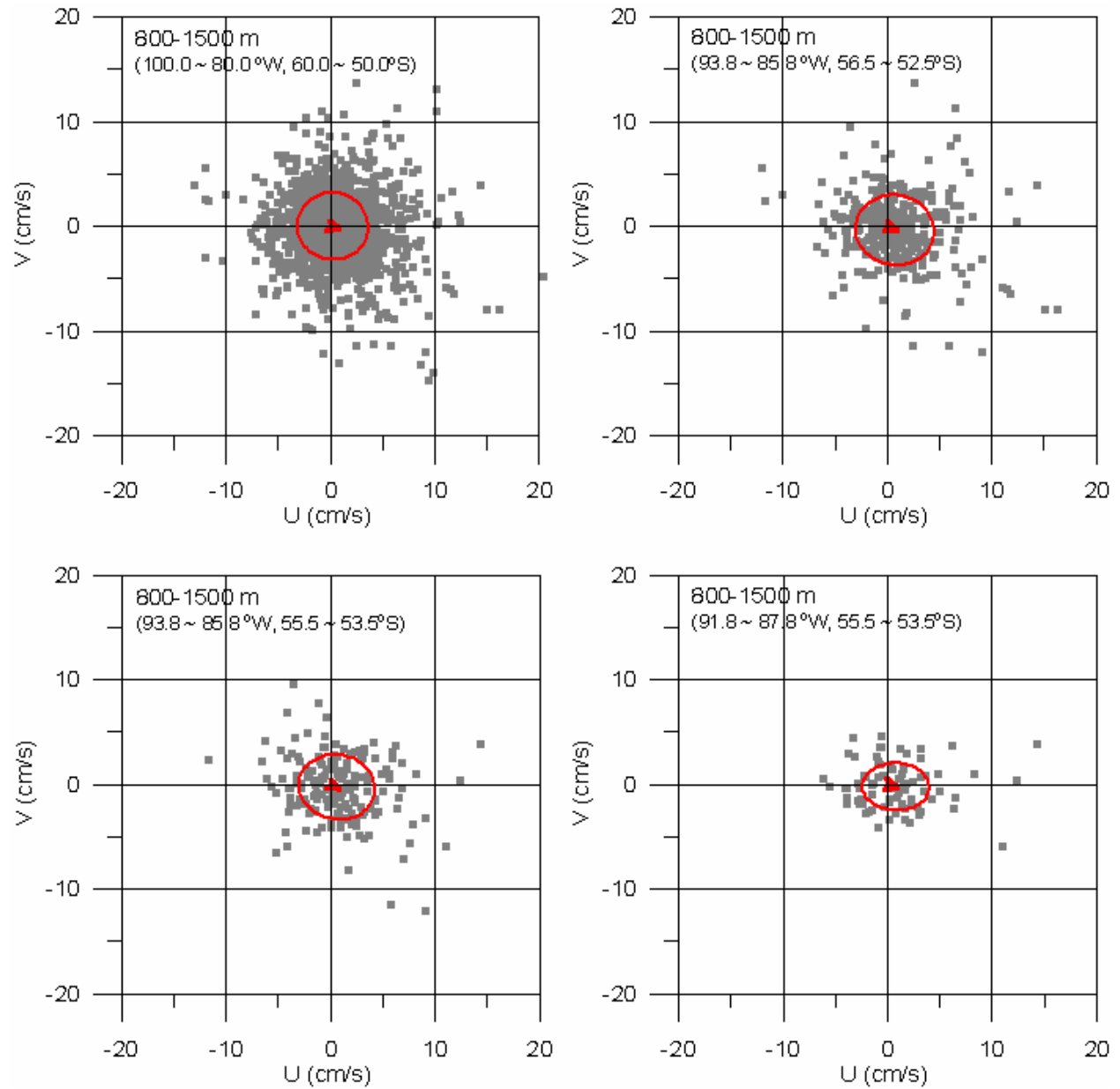


Figure 4. Scatter plot of horizontal currents derived from Argo floats in the vicinity of the OOI site. Different panels refer to different spatial extent around the OOI site. Mean and one standard deviation are marked with red arrows and ellipses, respectively.

The following table shows the statistics underlying the data of Figure 4:

(top left) 100.0 ~ 80.0 degW, 60.0 ~ 50.0 degS mean u (cm/s) : 0.63064 mean v (cm/s) : -0.18151 u std. dev. (cm/s): 3.4366 v std. dev. (cm/s): 3.4011	(top right) 93.8 ~ 85.8 degW, 56.5 ~ 52.5 degS mean u (cm/s) : 0.81869 mean v (cm/s) : -0.24472 u std. dev. (cm/s): 3.7705 v std. dev. (cm/s): 3.3315
(bottom left) 93.8 ~ 85.8 degW, 55.5 ~ 53.5 degS mean u (cm/s) : 0.66136 mean v (cm/s) : -0.39273 u std. dev. (cm/s): 3.732 v std. dev. (cm/s): 3.0838	(bottom right) 91.8 ~ 87.8 degW, 55.5 ~ 53.5 degS mean u (cm/s) : 0.7575 mean v (cm/s) : -0.1284 u std. dev. (cm/s): 3.6815 v std. dev. (cm/s): 2.160

1.2.1.2. Reconstructed Current Profile

For the purpose of designing the OOI moorings, the following vertical current profiles were determined. Computational details are explained in the Appendix. There are three current profiles, meant to represent three scenarios:

- Background field. Represents a one-RMS statistic.
- Eddy event. Represents a two-RMS statistic.
- Extreme event. Represents a three-RMS statistic.

Table 1 lists all three values, whereas Figure 5 shows only the background field and the underlying equation.

Table 1. Reconstructed current profiles for three scenarios, i.e. background field, eddy event, extreme event.

Pressure [dbar]	Background Field	Eddy Event	Extreme Event
	Current Speed [cm/s]	Current Speed [cm/s]	Current Speed [cm/s]
0	25.40	50.80	76.20
250	23.33	46.65	69.98
500	21.53	43.06	64.59
750	19.98	39.96	59.94
1000	18.63	37.27	55.90
1250	17.47	34.94	52.42
1500	16.47	32.93	49.40
1750	15.59	31.19	46.78
2000	14.84	29.68	44.52
2250	14.19	28.38	42.57
2500	13.63	27.25	40.88
2750	13.14	26.27	39.41
3000	12.71	25.43	38.14
3250	12.35	24.70	37.05
3500	12.03	24.07	36.10
3750	11.76	23.52	35.28
4000	11.52	23.04	34.57
4250	11.32	22.63	33.95
4500	11.14	22.28	33.42
4750	10.99	21.97	32.96
5000	10.85	21.71	32.56
5250	10.74	21.48	32.22
5500	10.64	21.28	31.92
5750	10.55	21.11	31.66
6000	10.48	20.96	31.44

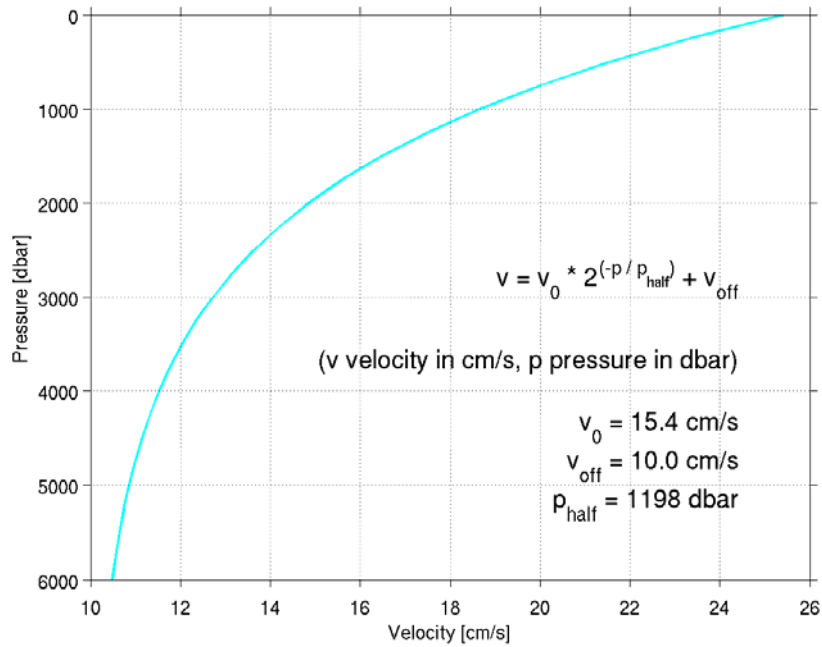


Figure 5. Background field of reconstructed current profile.

1.2.2 Mean Dynamic Ocean Surface Topography

The “mean dynamic ocean topography” (MDOT) is that part of mean sea surface height that actually drives currents, as opposed e.g., to elevation because of the geoid. Assuming that these mean currents are geostrophic, one can interpret the MDOT as a stream function for the currents, such that the currents are parallel to lines of constant MDOT, and that current strength is inversely proportional to the spacing of these lines. Hence, Figure 6 shows the mean circulation. From the MDOT product, the mean geostrophic surface current amounts to 2.0 cm/s for the Southern Ocean.

The 1992-2002 mean ocean dynamic topography data has been obtained from Nikolai Maximenko (IPRC) and Peter Niiler (SIO).

The Rio5 MDOT was produced by CLS Space Oceanography Division and distributed by AVISO [6], with support from Cnes.

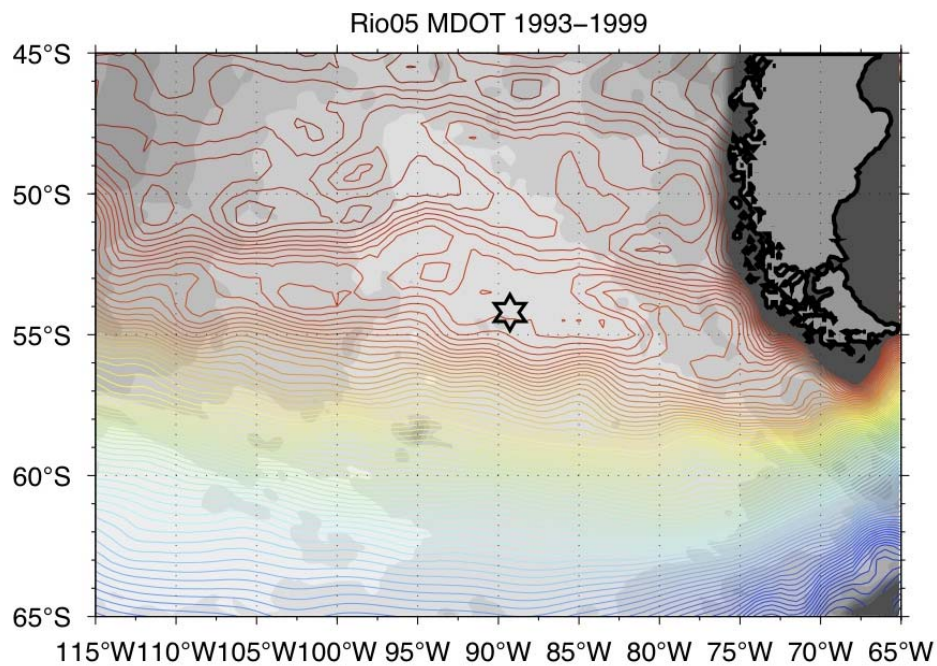
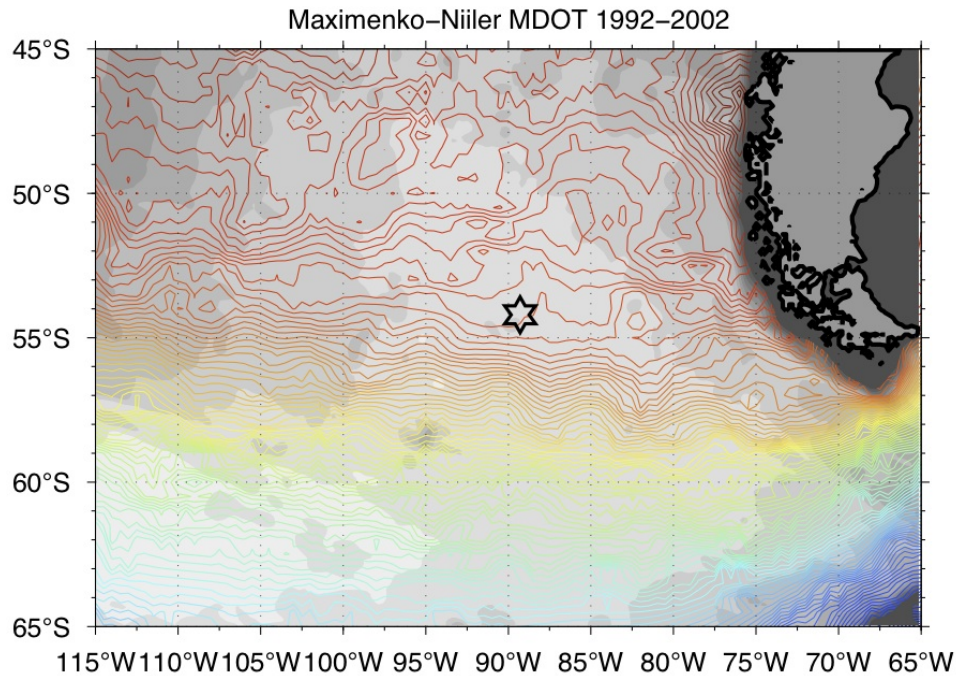


Figure 6. Comparing two different products for mean dynamic ocean topography at the Southern Ocean Global Array site (star symbol). Top: Product by Maximenko and Niiler (2005). Bottom: Product by Rio et al. (2005). Contours are 2 cm apart; gray shades show bathymetry every 500 m.

1.2.3 Sea Surface Height Variability

Variability of sea surface height (SSH) shows variability of the circulation. In Figure 7, it is computed as the standard deviation of SSH as measured by satellite altimetry, which makes it a proxy for Eulerian eddy kinetic energy (EKE). High values can be caused by passing eddies and meandering permanent currents, and are often (but not always) co-located with strong mean currents.

Altimeter products were produced by Ssalto/Duacs and distributed by AVISO [4], with support from Cnes.

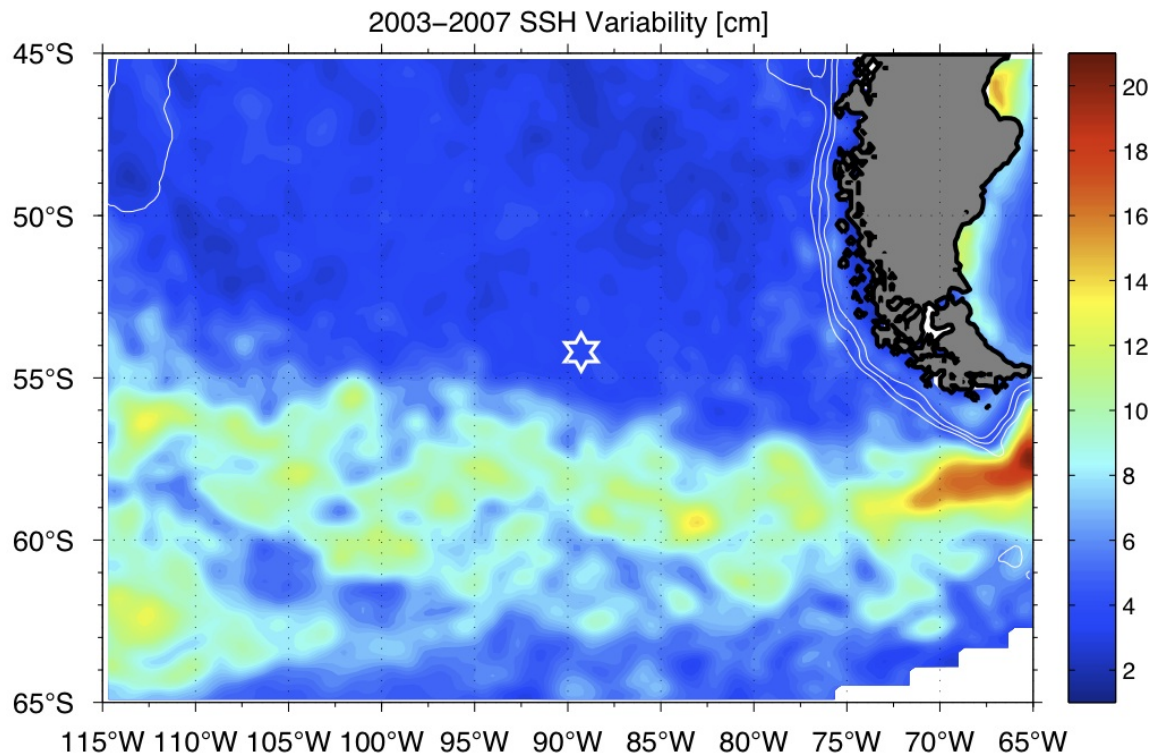


Figure 7. Variability of sea surface height from the AVISO global merged altimetry product, computed as standard deviation in cm. The star shows the Southern Ocean Global Array site. White lines show bathymetry at 3000, 2000, and 1000 m.

1.2.4 Baroclinic Rossby Radius

The baroclinic Rossby radius (Figure 8), or radius of deformation, is a property derived from stratification, i.e. from the density profile at a given location. It represents a (horizontal) distance. Theories of fluid instability (e.g., Eady theory) relate typical eddy sizes in the ocean to a multiple of this quantity.

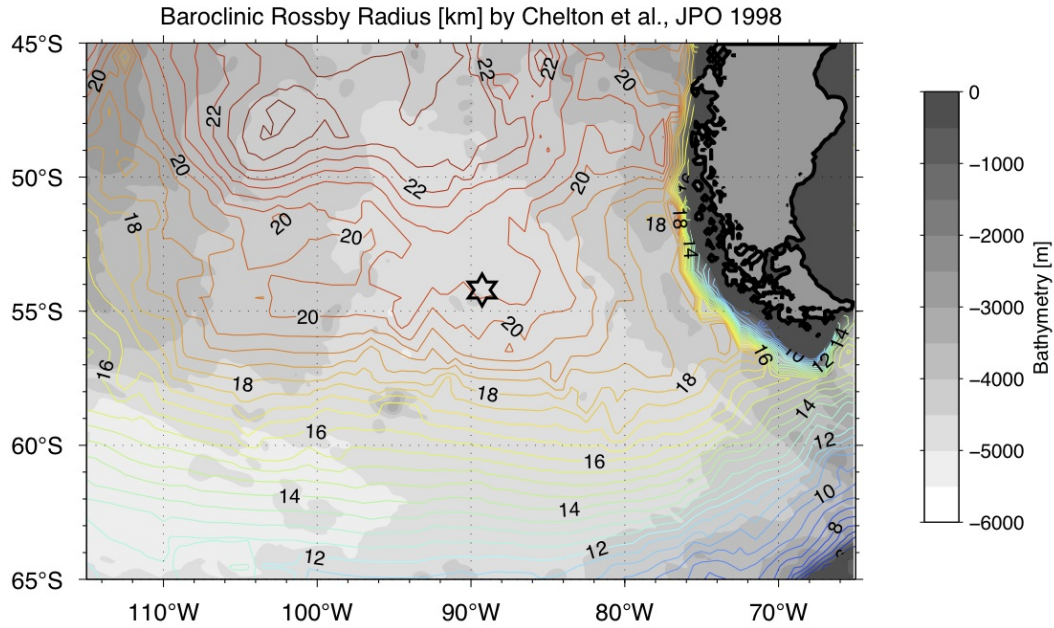


Figure 8. Rossby radius of deformation at the Southern Ocean Global Array site. Product by Chelton et al. (1998) [7]. Gray shades show bathymetry every 500 m.

1.2.5 Lagrangian Length Scale from Surface Drifters

Figure 9 shows the Lagrangian length scale derived from surface drifter data. This is another measure of typical eddy sizes, and it amounts to circa 20 km at the OOI site in the South Pacific.

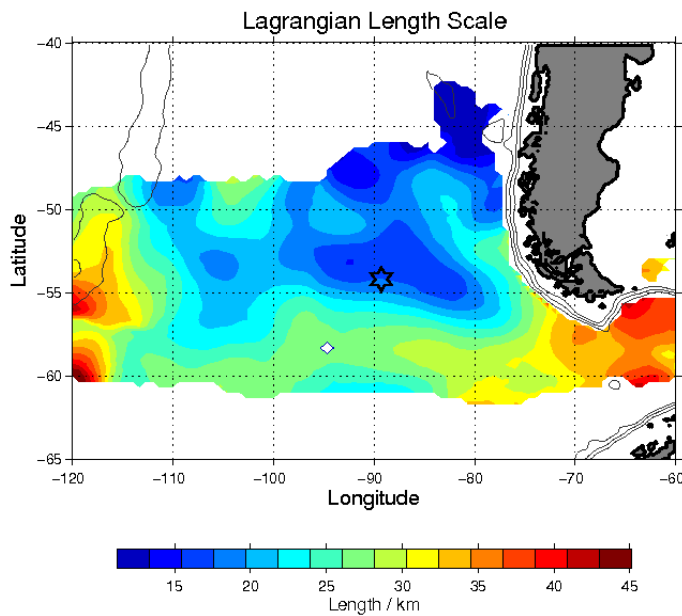


Figure 9. Lagrangian length scale computed from surface drifter trajectories.

1.3. Environmental Conditions

1.3.1 Historical Wind Data

Scatterometer data from satellites was a source of wind speed and wind direction for the Southern Ocean Site. The *Climatology of Global Ocean Winds (COGOW)*[8] is an interactive map-based database of daily averaged wind data. Data are available at a spatial resolution of 0.5° latitude/longitude, and daily temporal resolution. The data used here correspond to a 0.5° x 0.5° patch centered at 55.25° N and 89.75° W (Figure 11). Each daily value represents an average of measurements made in the bracketing 3-day interval. Data are currently available for the period January 1999 – December 2004.

Another data source used to characterize these sites is GROW hindcast data [9] (Global Reanalysis of Ocean Waves, from OceanWeather Inc.). This data is available at 3 hour resolution from 1995-2004. For the Southern Ocean Site, the data is available at Lat 55.0° S, 90.0° W (Figure 10). There is no clear seasonal trend in this data, in either the averages or the extremes (Figure 12). The yearly average instead is always around 20 knots.



Figure 10. Location of Southern Ocean Array (yellow triangle) COGOW site [8] (purple square), and GROW point 6560 (green circle). (Google Earth)

Figure 13 shows the comparison of the two data sets. There is a definite correlation, when the GROW data is represented with a 3-day running average. This suggests that at temporal scales longer than a day, statistics from any of the sources would accurately characterize climatological wind conditions at the Southern Ocean site.

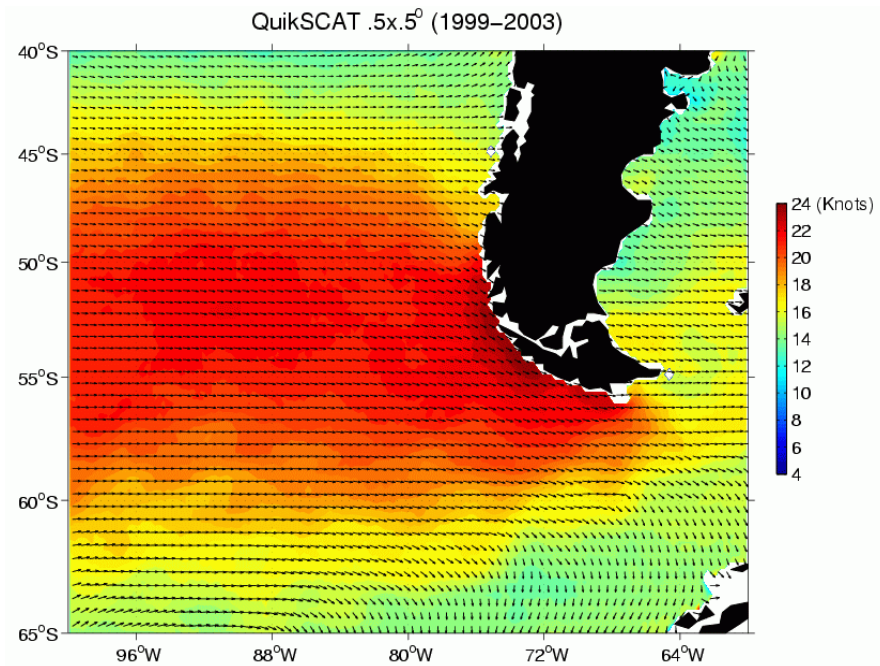


Figure 11. COGOW site at 55.25° S and 89.75° W. Each arrow represents daily averaged wind data from 1999-2004.

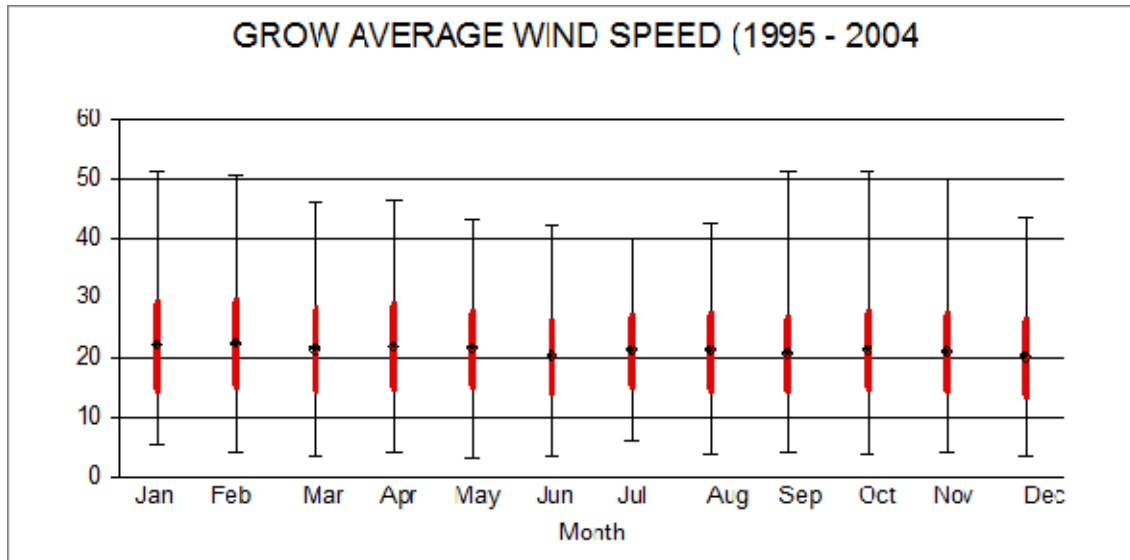


Figure 12. Monthly means, standard deviations, and extremes of hourly average wind speeds measured from GROW data [9].

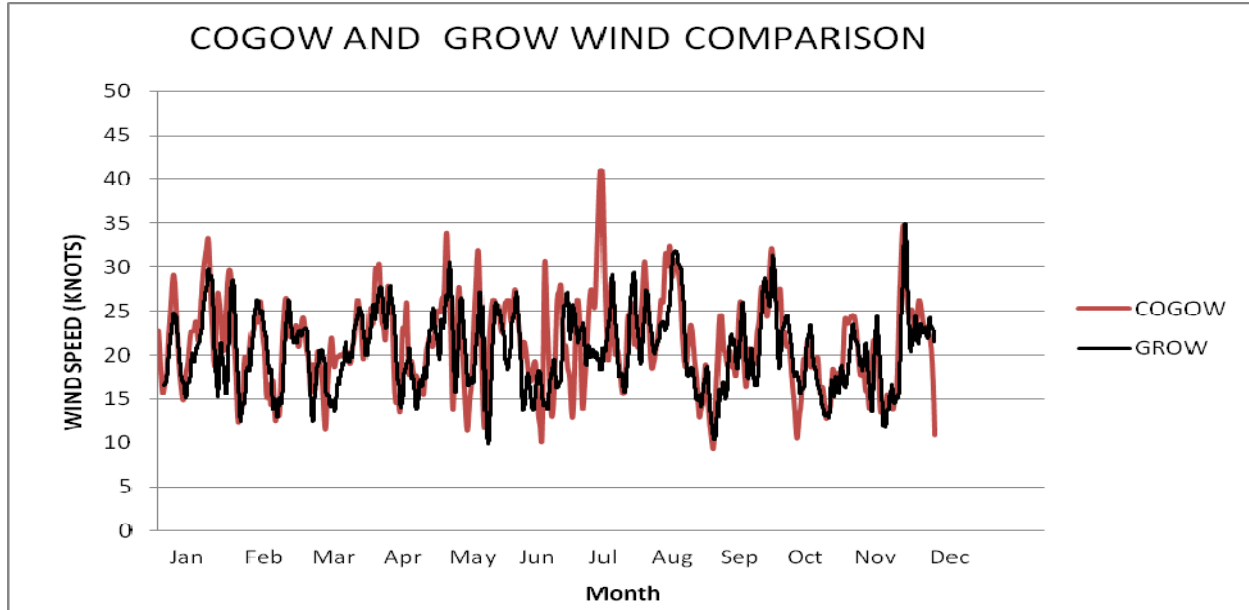


Figure 13. Wind speed measurements from the GROW data [9] and a COGOW [8] product based on NASA's QuikSCAT scatterometer [10] during a 7-month period in 2003 when data from all three sources are gap-free. The GROW data were fitted with a 3-day running mean for consistency with the satellite product.

From a QuikSCAT data product of three-day average wind values available at <http://www.remss.com> [11], the following are derived:

- Mean wind speed: 11.0 m/s
- Standard deviation of wind speed: 2.8 m/s

These QuikScat data are produced by Remote Sensing Systems and sponsored by the NASA Ocean Vector Winds Science Team.

1.3.2 Historical Wave Data

GROW (Global Reanalysis of Ocean Waves, [9]) was used to characterize the significant wave height data for the Southern Ocean Site at 55.0° N, 90.0° W. This data is available at 3 hour resolution from 1970-2005. There is no a clear seasonal trend (Figure 14). The extremes of 11-16 m waves are present in all months. Storm peak data is also plotted in Figure 15. The storm threshold for significant wave height is 8 m.

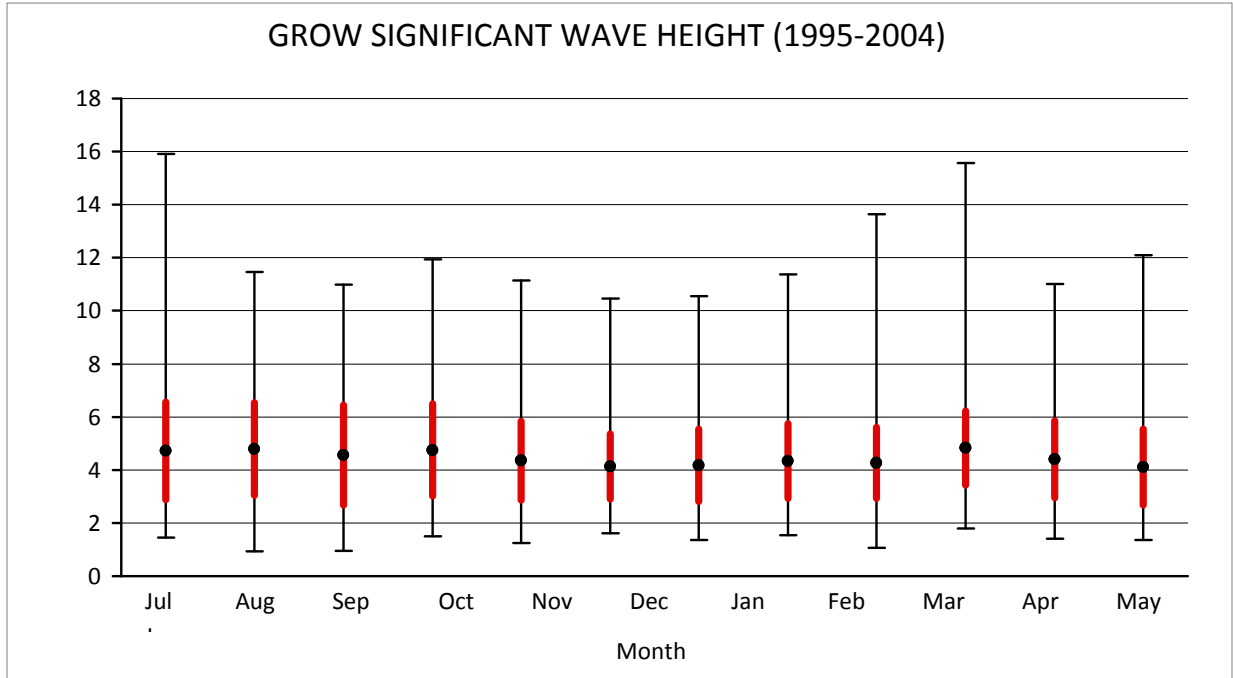


Figure 14. Monthly means, standard deviations, and extremes of significant wave height provided by GROW data [9].

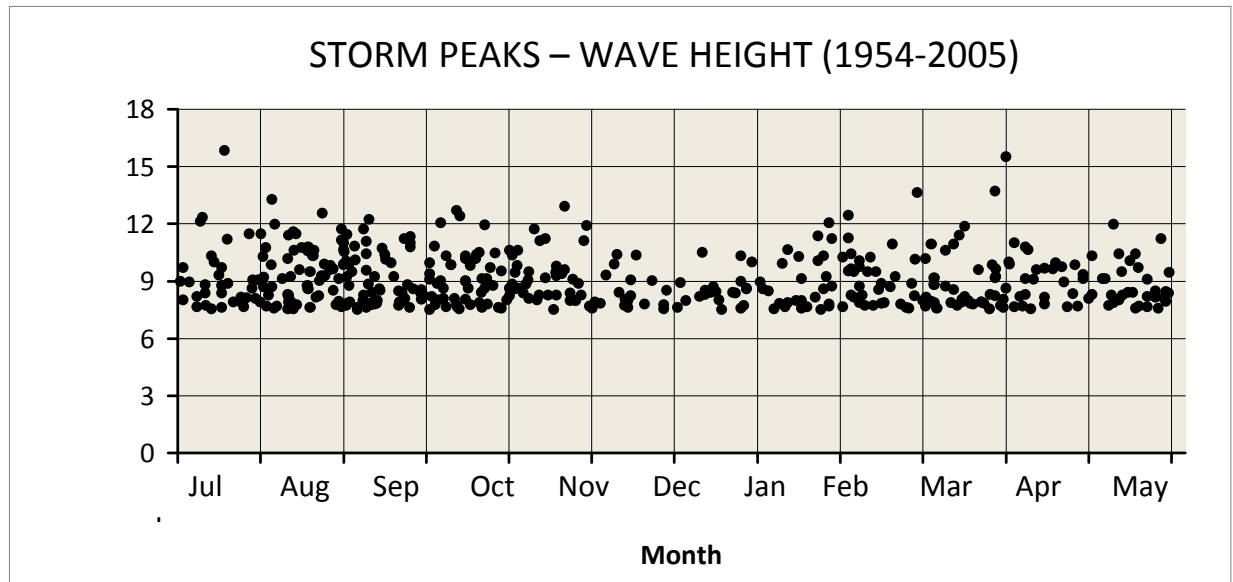


Figure 15. GROW Storm peak data for significant wave height.

1.3.3 Weather Extremes

The significant wave height and sustained wind for 10 year, 30 year, and 100 year events are estimated from wave and wind records from GROW hindcast data (see Appendix A for details of the analysis). The wave and wind records were compiled from January 1970 – December 2004, representing 35 years of data.

Table 2. Wind and wave extremes

	Significant Wave Height (m)	Peak Period (s)	Wind Speed (m/s)
10 Year Return Period	13.9	18.6	28.5
30 Year Return Period	15.0	19.4	30.1
100 Year Return Period	16.0	20.2	31.7

1.3.4 Solar Radiation

The Atmospheric Science Data Center at NASA Langley provides a number of satellite-derived data products relating to surface meteorology and solar energy. Data is available with a horizontal resolution of 1° in latitude and longitude. Table 2 shows monthly averages of solar radiation incident on a horizontal surface for the 22-year period July 1983-June 2005. Higher resolution daily data sets are also available.

Another Source is the PG&E solar radiation model based on the ASHRAE model [12] (<http://www.pge.com/mybusiness/edusafety/training/pec/toolbox/arch/calculators.shtml>). This model is widely used by the engineering and architectural communities (ASHRAE handbook: HVAC applications). Since this model only accounts for direct normal irradiance, the data was scaled down with a cloud cover factor by 30%, to make it comparable to real data as well as the NASA satellite data (Figure 16). During the 12 month time scale, the two data sets overlap within 15%, a reasonable agreement (Table 2). The seasonal cycle of insolation is clearly seen, with maximum average near 250 W/m² and average minima near 15 W/m².

Table 3. Monthly Averaged Insolation on a Horizontal Surface (W/m²) at 54.26° S, 89.28° W.

	Jan	Feb	Mar	Apr	May	Jun	Jul	Aug	Sep	Oct	Nov	Dec
NASA	220.4	170.4	115.0	67.1	32.5	20.0	26.3	53.3	98.3	157.1	210.4	235.0
PG&E CLOUD	247.4	196.4	129.2	67.5	29.4	14.9	20.2	47.4	98.7	165.2	227.8	261.4

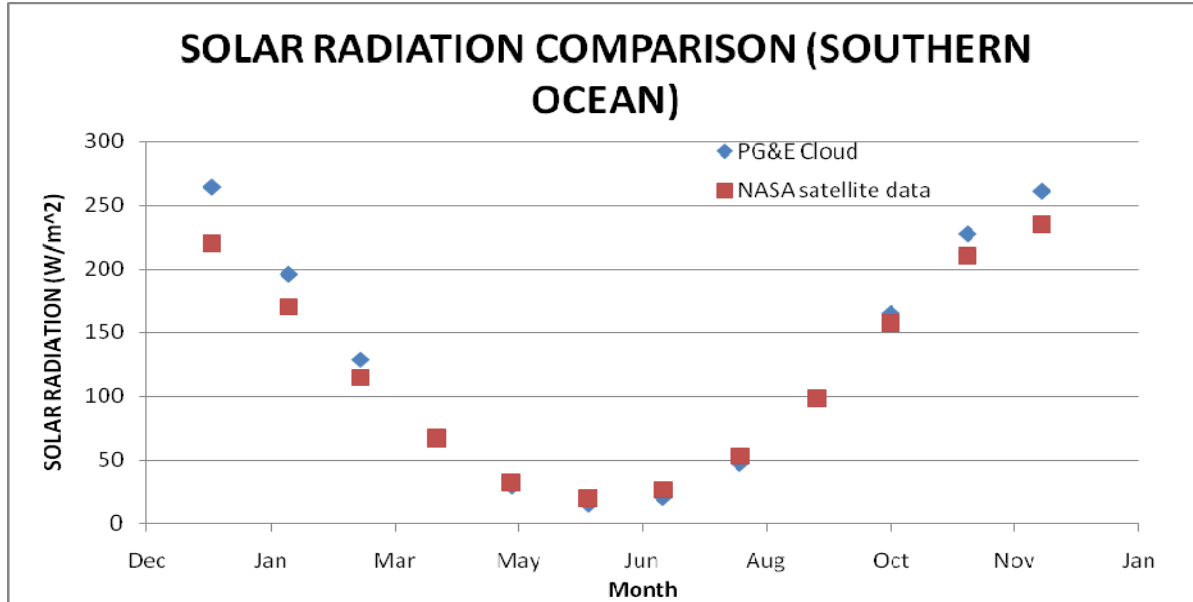


Figure 16. Solar Radiation Comparisons between the Atmospheric Science Data Center at NASA Langley satellite-derived data [13] and the PG&E/ASHRAE model data [12] reduced by 30% to compensate for Cloud Cover.

Histograms of average daily insolation taken from the PG&E model reduced by 30% to compensate for cloud cover for one year for 55°S, 90°W are shown by month in Figure 17. Winter months (May-Aug) show relatively compact distributions, with mean insolation near 100 W/m². Distributions are qualitatively different in spring and summer (Oct-Feb), when long tails are seen on the low end of the distribution. Peaks in the spring and summer distributions occur at values between about 500 W/m² and 600 W/m².

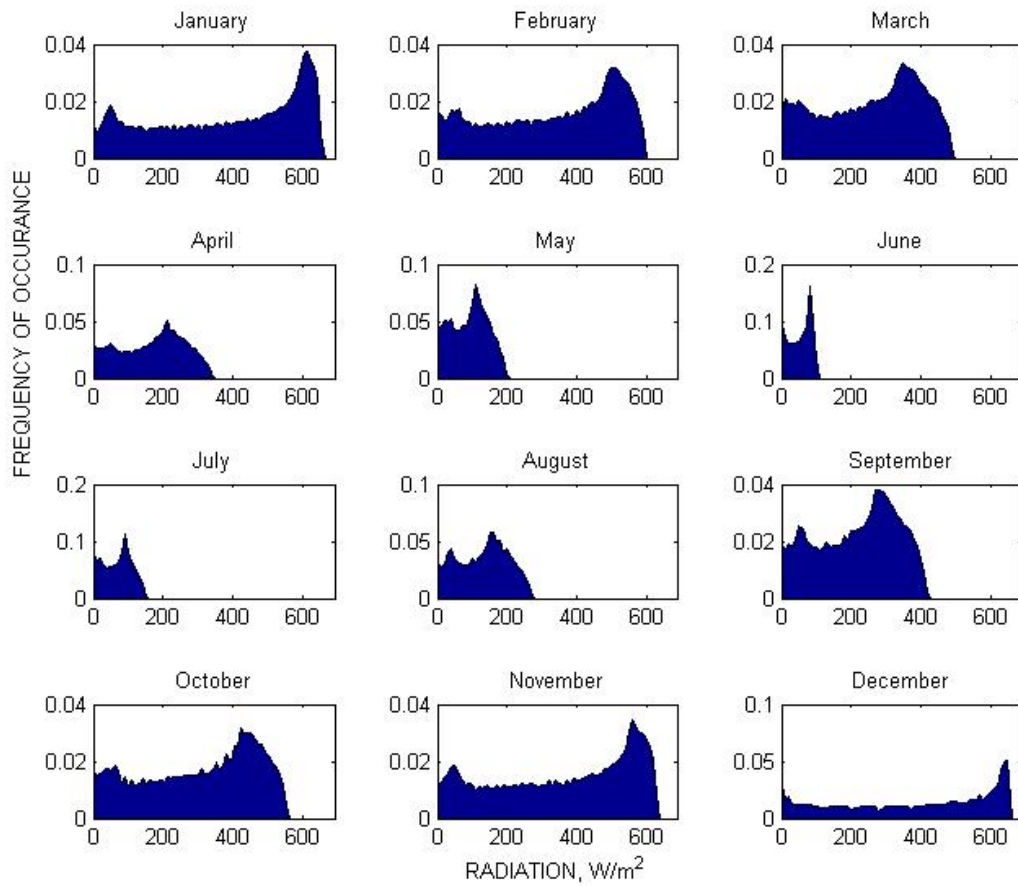


Figure 17. Monthly distributions of daily average isolation on a horizontal surface given by the PG&E model data reduced by 30% to account for cloud cover.

1.4. Commercial/Policy Factors

1.4.1 Shipping Lanes

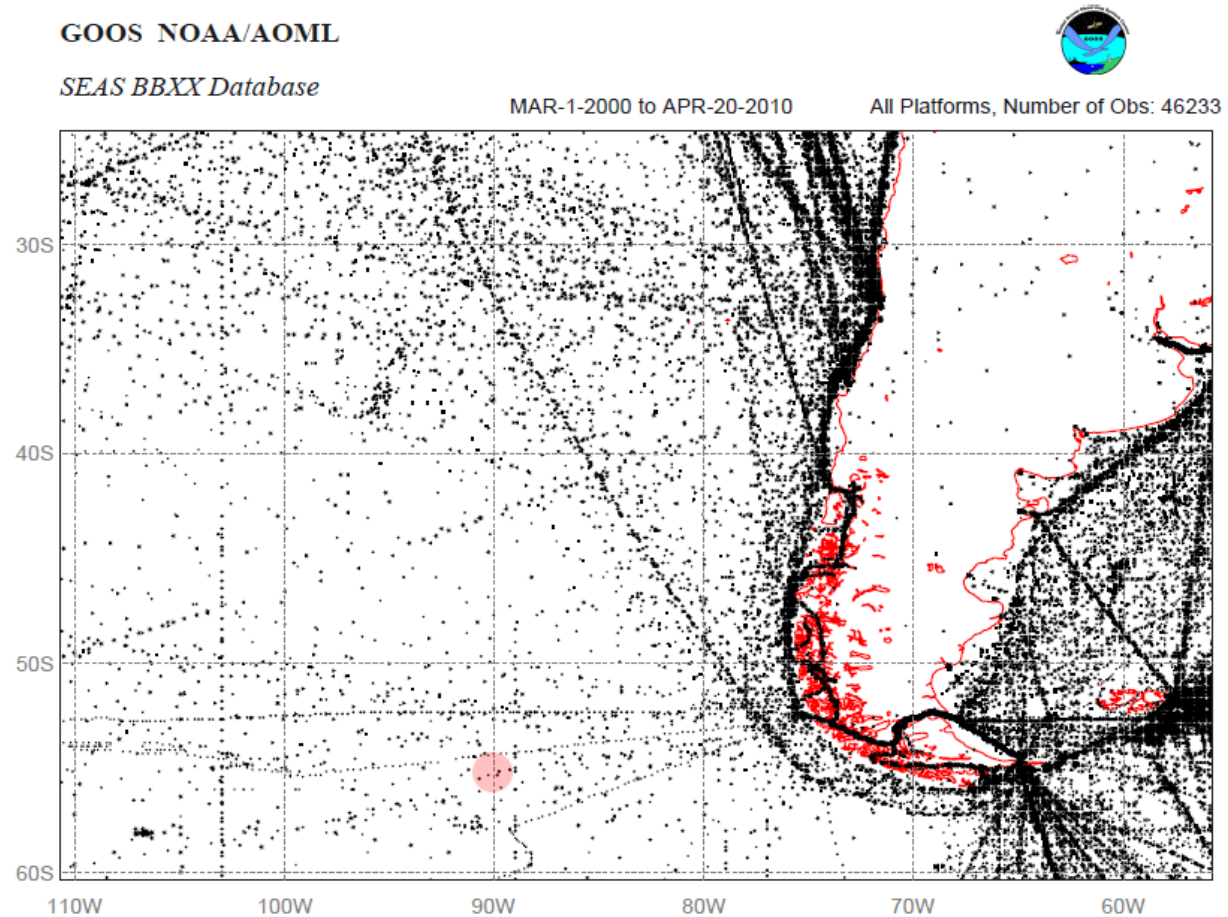


Figure 18. National Oceanic and Atmospheric Administration (NOAA) satellite data transmission locations from SOOP (Ship of Opportunity) vessels. Note: Transparent red circle at 55°S, 95°W indicates location of the Southern Ocean Array. Product courtesy of: NOAA BBXX, Joaquin A. Trinanes [14].

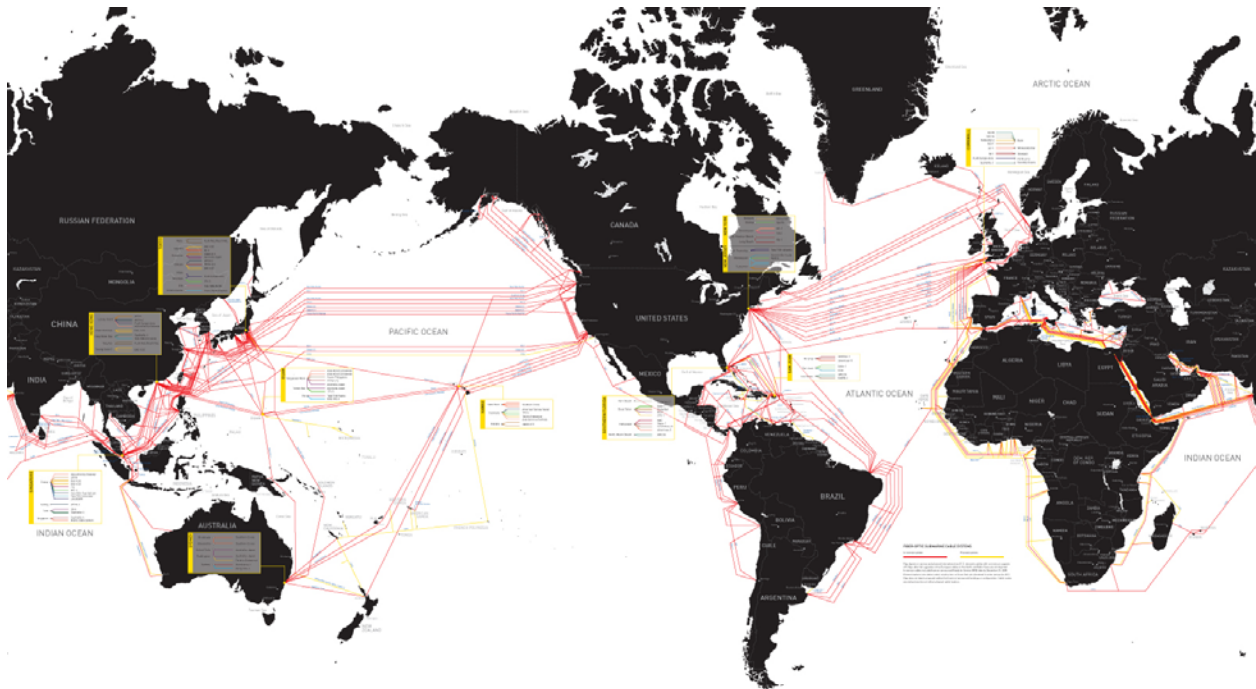
Figure 18 displays satellite acquired ship position for ships participating in the NOAA SOOP (Ship of Opportunity) data collection program. This data covers all transmission points from SOOP vessels over a 10 year period beginning 1 Mar 2000 and ending 20 April 2010. Vessel types participating include merchant vessels, fishing vessels, US Coast Guard and NOAA vessels. A “commercial shipping” dataset listing the number of large ships recorded, by satellite observation, in each 1-km² of the world ocean for a 12-month period starting in October 2004 available from the National Center for Ecological Analysis and Synthesis at UC Santa Barbara [15] confirms the shipping traffic patterns displayed in Figure 18. Based on these two datasets, the Southern Ocean Global Observatory is outside the most frequently used shipping paths.

1.4.2 Fishing Areas

The Southern Ocean Array is located in FAO Fishing Area 87.3.3 (www.fao.org [16]). It is north and outside of the region monitored by the Convention on the Conservation of Antarctic Marine Living Resources (CCAMLR) – FAO Fishing Areas 48, 58, and 88 (www.ccamlr.org [17]). The Southeastern Pacific is predominately fished by Chile and Peru, with perch-like fishes as the primary catch (Sea Around Us Project [18]).

1.4.3 Seafloor Cables

Figure 19 shows the global network of submarine telecommunications cables. The SAM-1 submarine telecommunications cable is owned by Telefonica International Wholesale Services (TIWS). The southern-most landfall of this cable system in the Pacific Ocean is Valparaiso, Chile. It is approximately 2750 km northeast of the Southern Ocean Array.



TeleGeography's
Global Submarine Cable Map 2010

Figure 19. Global map of submarine telecommunication cables.

1.4.4 Other Moorings

At present no other moorings are known to be located in the Southern Ocean Array area.

1.4.5 Satellite altimetry tracks

The global OOI site locations were chosen to be co-located with crossing ground tracks of present satellite altimeters. As of 2010, this orbit is occupied by the Jason-2 satellite (previously Jason-1 and TOPEX/Poseidon). Figure 20 shows spatial SSH correlation to obtain an independent estimate of typical eddy sizes.

Along-track altimetry data were obtained from NASA's Physical Oceanography Distributed Active Archive Center (PO.DAAC, [19]).

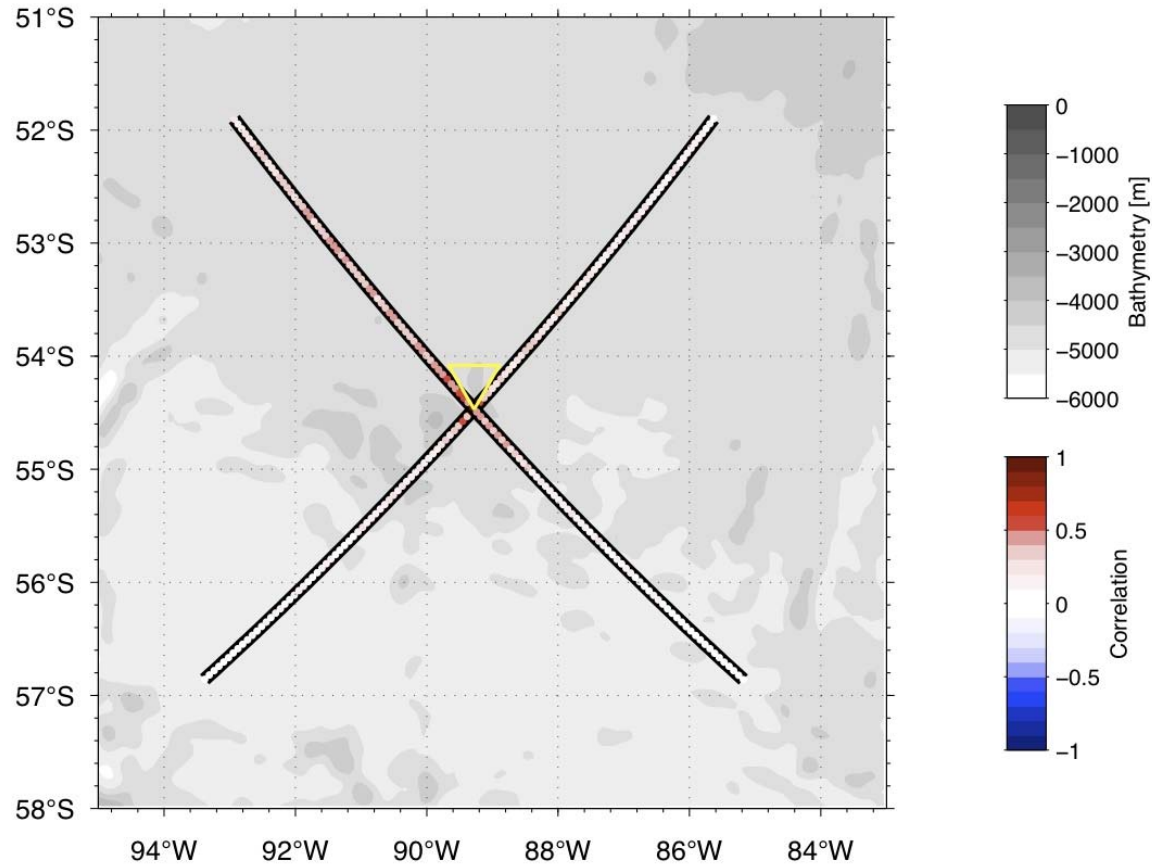


Figure 20. PRELIMINARY: Spatial correlation in along-track sea surface height anomaly as seen by satellite altimetry. Data are from the TOPEX/Poseidon satellite, cycles 12 through 364, in an along-track gridded product obtained from PO.DAAC (<http://podaac.jpl.nasa.gov>, [19]) and have been high-pass filtered at about 180 days to highlight the mesoscale eddy field.

2. Site Design

2.1. Site Components

The Southern Ocean Array consists of four moorings: a Surface Mooring, a Hybrid Profiler Mooring, and two Subsurface Flanking Moorings.

- The **Surface Mooring** is an inverse catenary mooring with a high power Global Surface Buoy at the top and an anchor at the bottom. The watch circle of the Surface Mooring is 4.24 km and is calculated from the scope of the mooring ($1.25 \cdot \text{depth}$) and the stretch of the nylon portions of the mooring line.
- The **Hybrid Profiler Mooring** consists of a taut subsurface mooring with a wire-following profiler, and a subsurface platform at ~230 m depth from which a surface-piercing profiler is deployed.
- The **Flanking Moorings** are taut subsurface moorings with a sub-surface float at ~30 m depth.

2.2. Site Configuration

2.2.1 Moored Array

The moored array will be configured as an equilateral triangle with one corner pointing poleward. The mooring locations described below are based primarily on Smith & Sandwell global bathymetry [3] (general array location), Rossby radius (length of array sides), and satellite altimetry track lines (orientation of array). During the first deployment cruise, high-resolution multi-beam bathymetry surveys will be made of the deployment region. The actual mooring locations will be based on the results of that survey which may reveal the presence of seamounts or holes.

For the Southern Ocean Array, the Surface Mooring will be located at 54.4704° S , 89.2796° W (Figure 21). The Hybrid Profiler Mooring will be located 7.1 due north from the Surface Mooring, and Flanking Moorings A and B will be located 50 km (PRELIMINARY) from the Surface Mooring due 330 and 30 degrees, respectively (Table 3, and Figure 21b). The appropriate spacing between the Surface Mooring and the Hybrid Profiler Mooring was calculated from the watch circles of both moorings (4.24 km and 10% of depth, respectively), plus an additional 50% to account for uncertainties in mooring placement (Figure 22).

The positions of the moored array are described by three parameters:

- *Site Center*. This is the central location for a site, from which the Site Radius is measured. The Site Center is listed in array location tables and plotted on maps. However, the mooring or moorings at the site may not be located at the Site Center. They will be located within the Site Radius.
- *Site Radius*. This is the region within which the mooring at each site will be located. A region, rather than an exact location, is necessary to allow for local-scale bathymetric features unresolved on available maps, uncertainties in “anchor-over” position, anchor fall-back during deployment, and the possibility that a replacement mooring may be deployed before the original mooring is recovered. The Site Radius is two times the nominal depth of the array.

- *Mooring Separation.* This is the distance between mooring anchor positions, described relative to the Surface Mooring position. The Hybrid Profiler Mooring is located as close to the Surface Mooring as possible (as described above). The Flanking Mooring separations, which can also be thought of as the length of the “sides” of the triangular array are based on the length-scale of mesoscale features in the region. Actual mooring positions and separations will only be known after deployment.

Table 4. PRELIMINARY: Mooring Locations

	Depth	Site Center		Site Radius	Mooring Separation
		Latitude	Longitude		
Surface Mooring GS01SUMO	~4800 m	54.4704° S	89.2796° W	9.6 km	
Hybrid Profiler Mooring GS02HYPM	~4800 m	54.4068° S	89.2796° W	9.6 km	7.1 km from Surface Mooring
Flanking Mooring A GS03FLMA	~4800 m	54.0814° S	89.6652° W	9.6 km	50 km from Surface Mooring
Flanking Mooring B GS03FLMB	~4800 m	54.0814° S	88.8940° W	9.6 km	50 km from Surface Mooring

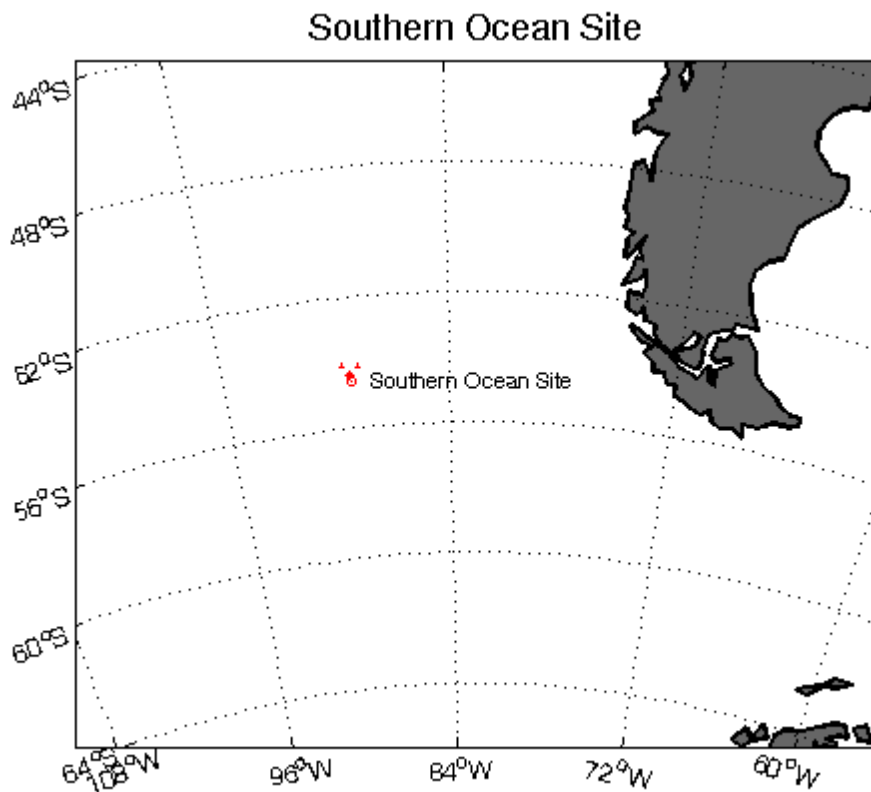


Figure 21a. Location of the Southern Global Array.

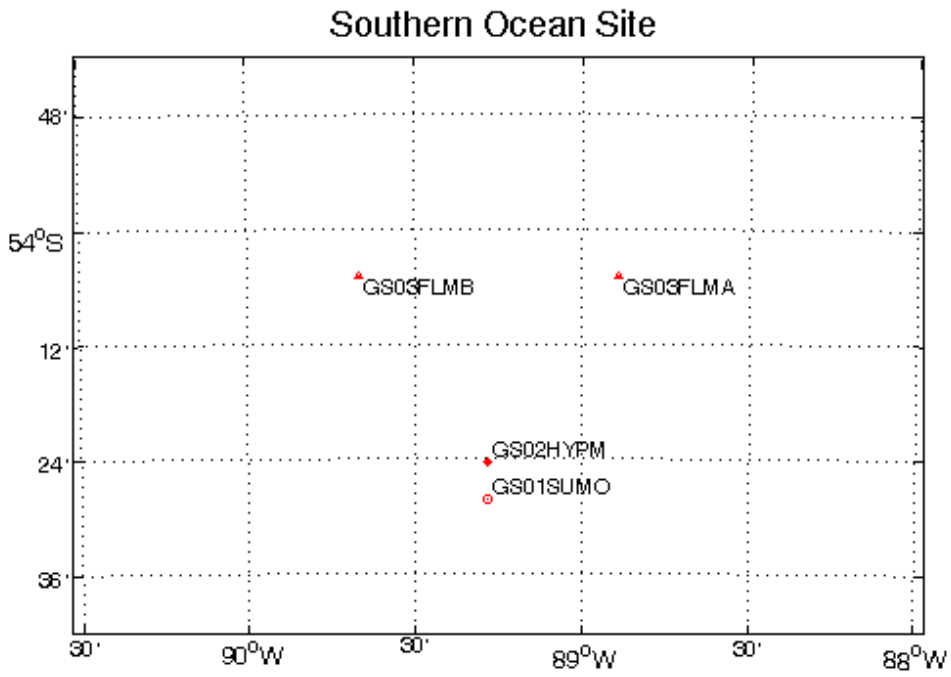


Figure 21b. Layout of the Southern Global Array.

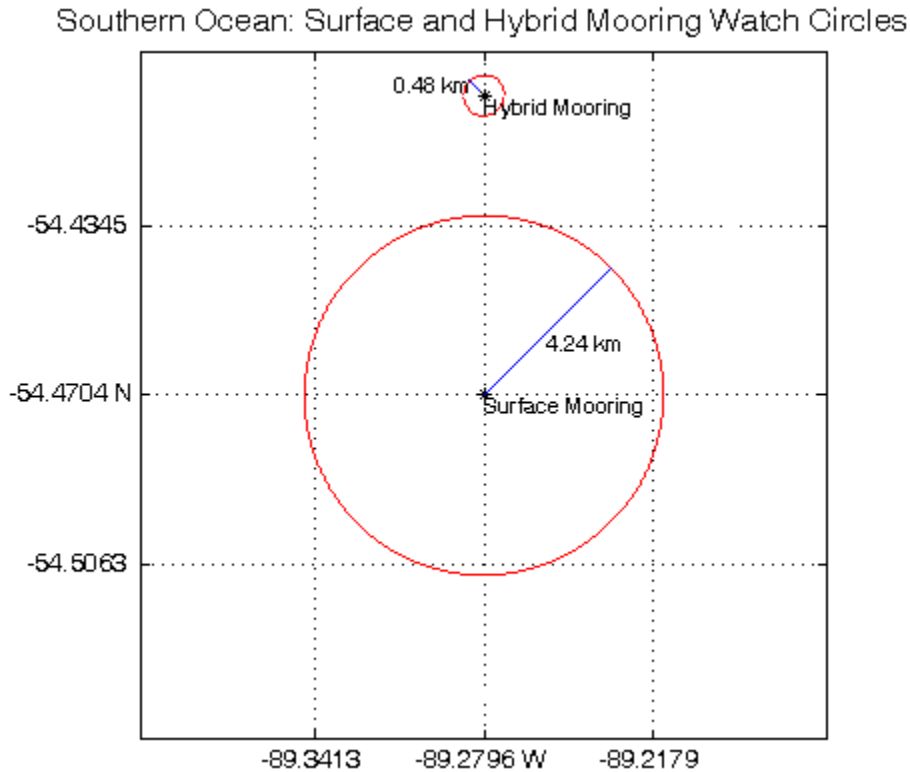


Figure 22. The spacing between the Surface Mooring and the Hybrid Profiler Mooring is 7.080 km. This spacing takes into account the watch circles of both moorings (red circles), and other uncertainty factors such as deployed mooring location.

2.2.2 Glider Operations Area

Three open ocean gliders will operate in the vicinity of the moored array. The default mission plan of the gliders is to profile the water column from 1000 m depth to the surface in paths between the Surface Mooring and the Flanking Moorings. This will provide greater horizontal context to better resolve mesoscale features. The gliders will also provide adaptive sampling capabilities to respond to events in the area.

3. References

Chelton, D.B., R. A. deSzoeko, M. G. Schlax, K. El Naggar and N. Siwertz, 1998. Geographical variability of the first-baroclinic Rossby radius of deformation. *J. Phys. Oceanogr.*, 28, 433-460. <http://www.coas.oregonstate.edu/research/po/research/chelton/index.html>

England, M. H., J. S. Godfrey, A. C. Hirsy, and M. Tomczak, 1993. The mechanism for Antarctic water renewal in a world ocean model. *J. Phys. Oceanogr.*, 23, 1553-1560.

Maximenko, N. A. and P. P. Niiler. *Recent Advances in Marine Science and Technology* (Ed.: N. Saxena), chapter Hybrid decade-mean global sea level with mesoscale resolution. PACON International, 2005.

Rio, M.-H. , P. Schaeffer, F. Hernandez, and J.-M. Lemoine. The estimation of the ocean Mean Dynamic Topography through the combination of altimetric data, in-situ measurements and GRACE geoid: From global to regional studies. In *Proceedings of the GOCINA international workshop, Luxembourg, 2005*.

Sabine, C., L., N, Gruber, R.M Key, K. Lee, J. L. Bullister, R. Wannikopf, C. S. Wong, D. W. R. Wallace, B. Tillbrook, F. J. Millero, T-H Peng, A. Kozyr, T. Ono, and A. F. Rios, 2004. The oceanic sink for anthropogenic CO₂, *Science*, 5682, 367-371.

Appendix A. Methodology for determining extreme events

10, 30, and 100-Year Sea States

Historical records for significant wave heights come mostly from reanalysis of wind data collected by satellites. The wind data is used as input into numerical models that calculate significant wave height. Since winds are averaged over a fairly coarse grid, the significant wave heights typically underestimate short-term events as measured by surface buoys. In one instance (**Station Papa**), we are able to compare 35-year results from GROW data reanalysis to overlapping 25-year measurements from an NDBC surface buoy (46001). The GROW data reanalysis underestimates 10,30, and 100-year sea states by about 10%.

Extreme events (10, 30, and 100-year sea states) are estimated using Peak-Over-Threshold method. We catalogue the peaks above a given threshold (typically 0.5 to 0.75 of the maximum significant wave height of the given time record). The peaks we choose must be separated by at least 48 hours (this is our subjective criteria to insure independent storm events). If there are two peaks within a ± 48 -hour window, then we only retain the largest peak within the window. We calculate the cumulative probability distribution for the peaks above our threshold such that $\Pr(H_s \leq H_t) = 0$ where H_s is the significant wave height and H_t is the threshold and $\Pr(H_s \leq H_m) = 1 - 1/(N+1)$ where H_m is the maximum peak and N is the total number of peaks above the threshold. Generalized Pareto Distributions are fitted to the measured distributions corresponding to different thresholds. Goodness of fit criteria is applied to the different threshold distributions, and this used to determine the parameters for the Generalized Pareto Distribution to use in estimating 10, 30, and 100-year sea states. The input cumulative probability for a N -year sea state is given by $1-1/(N*m)$ where m is the average number of peaks per year above the given threshold.

10, 30, and 100-Year Wind

Extreme wind events are determined in the same manner using Peak-Over-Threshold method. The wind data comes from satellite reanalysis studies and from surface buoy measurements.

Current Profiles

Consistently estimating typical current profiles for the four global-ocean OOI sites is made difficult by different levels of data availability/sparsity between the sites. To overcome this, current speed profiles were constructed for each site as vertically decaying exponentials plus an additional offset. The parameters to describe these functions are: the offset, the exponential decay depth, and the exponential initial value.

The offset was chosen to be 10 cm/s for all sites.

The vertical 50%-decay depth of the exponential was derived for each site individually. It stems from the shape of the first baroclinic mode of horizontal velocity, which in turn is based on temperature and salinity profiles in the "World Ocean Atlas [20]" climatology. Values range approximately from 500m to 1200m.

The initial value of the exponential near the surface was chosen for each site individually, such that the velocity values would match those derived from an average of nearby surface drifter data and altimetry-derived surface currents, times a factor that makes these match near-surface ADCP values at the Irminger Sea site where such ADCP data exist.

The current speed values used for the ADCP, drifters, and altimeter were one-RMS values, which are thought of as representing the background field. Two stronger profiles were obtained by multiplying these with two and three, respectively interpreted as a typical eddy event and a multi-year repeat-cycle extreme event.

Appendix B. Data sources

1. Antarctic Intermediate Water formation in the southeast Pacific
<http://www-pord.ucsd.edu/~ltalley/aaiw/>
2. Ocean South Pacific Array
http://ioc.unesco.org/goos/MS/rpts/Chil_R99.htm
3. Smith, W.H.F., and D. T. Sandwell, *Global seafloor topography from satellite altimetry and ship depth soundings*. http://topex.ucsd.edu/marine_topo/ Science. **277**: p. 1957-1962.
4. Surface drifter data
<http://www.aoml.noaa.gov/envids/gld/>
5. Argo data centers
<http://www.argo.ucsd.edu>
6. Ssalto/Duacs altimeter products
<http://aviso.oceanobs.com/duacs/>
7. Global Atlas of the First-Baroclinic Rossby Radius of Deformation and Gravity-Wave Phase Speed (D. Chelton, OSU):
<http://www.coas.oregonstate.edu/research/po/research/chelton/index.html>
8. Climatology of Global Ocean Winds (COGOW) (OSU)
<http://numbat.coas.oregonstate.edu/cogow/>
9. GROW hindcast data was obtained from Oceanweather, Inc.
<http://www.oceanweather.com/>
10. QuikSCAT /SeaWinds Data Products
<http://manati.orbit.nesdis.noaa.gov/datasets/QuikSCATData.php/>
11. QuikSCAT wind data
<http://www.remss.com>
12. PG&E solar radiation model based on the ASHRAE model
<http://www.pge.com/mybusiness/edusafety/training/pec/toolbox/arch/calculators.shtml>
13. NASA Langley satellite-derived data
<http://eosweb.larc.nasa.gov>
14. SEAS BBXX & GTS AOML Database
<http://www.aoml.noaa.gov/phod/trinanes/BBXX/>
15. National Center for Ecological Analysis and Synthesis at UC Santa Barbara
<http://www.nceas.ucsb.edu/globalmarine/impacts>
16. Food and Agriculture Organization of the United Nations
<http://www.fao.org/>

17. Convention on the Conservation of Antarctic Marine Living Resources
<http://www.ccamlr.org/>

18. Sea Around Us Project
<http://www.searoundus.org/data/>

19. NASA Physical Oceanography Distributed Active Archive Center (PO.DAAC)
<http://podaac.jpl.nasa.gov/>

20. World Ocean Atlas
<http://www.nodc.noaa.gov/OC5/indprod.html>